Mon. Not. R. Astron. Soc. **299,** L25–L28 (1998)

HE 1127–1304: the largest radio quasar

Sanjay Bhatnagar,[1⋆] Gopal-Krishna[1⋆] and L. Wisotzki[2⋆]
[1]*National Centre for Radio Astrophysics, TIFR, Poona University Campus, Pune 411007, India*
[2]*Hamburger Sternwarte, Gojensbergsweg 112, D-21029, Germany*

Accepted 1998 June 25. Received 1998 June 15; in original form 1998 April 2

ABSTRACT

We report the discovery of a giant radio structure associated with the quasar HE 1127−1304 at $z = 0.6337$, found in a programme of radio follow-up of the Hamburg–ESO survey for bright QSOs in the southern sky. With a size of 2.4 Mpc, this is the largest known radio quasar as well as the largest radio source known at its redshift and beyond. The optical spectrum of this quasar shows an exceptionally deep Mg II absorption line at $\lambda_{\rm rest} = 2798$ Å.

Key words: intergalactic medium – quasars: general – radio continuum: galaxies.

1 INTRODUCTION

Following the discovery of megaparsec-sized giant radio sources (GRS) almost a quarter of a century ago, it was realized that such objects can be a useful probe of the intragalactic medium (IGM) and its evolution with redshift, z (Willis, Strom & Wilson 1974; Saunders 1982; Gopal-Krishna, Wiita & Saripalli 1989; Subrahmanyan & Saripalli 1993). This is feasible because the radio lobes of such sources extend well beyond any hot gaseous coronae associated with their parent galaxies. Until recently, discoveries of GRS were ususally not based on well-defined samples of candidates and hence they were less suitable for quantitative statistical studies. During the past few years, however, attempts have been made to build an unbiased sample of giant radio sources via optical follow-up of GRS candidates selected from the 7C survey (Cotter, Rawlings & Saunders 1996). This led to the discovery of five GRS with dimensions between 1 and 1.5 Mpc, all of which are identified with galaxies. It is also noteworthy that these GRS are located at relatively high redshifts ($0.4 \leq z \leq 0.9$), in contrast to the GRS discovered previously.

According to the currently popular unified scheme, the main axes of radio galaxies are preferrenially oriented closer to the plane of the sky, as compared to those of quasars (e.g. Barthel 1989). If this is the case, one would expect a dominance of radio galaxies in the samples selected on the criterion of large (projected) radio size. This is borne out by the optical identification statistics of an unbiased sample of radio sources with dimensions exceeding 0.7 Mpc; only two out of 13 GRS are identified as quasars, the remaining being galaxies (e.g. Cotter et al. 1996). The largest quasars reported thus far are 4C74.26 ($z = 0.104$: Riley et al. 1988) and 4C34.47 ($z = 0.2055$: Jägers et al. 1982, Barthel 1987), with apparent sizes of 1.5 and 1.8 Mpc, respectively. Here we report the discovery of a quasar at $z = 0.6337$ with an apparent radio size of 2.37 Mpc, which makes it the largest radio quasar known. This giant source has been discovered in the course of our continuing programme of radio follow-up of the Hamburg–ESO Survey (HES) which is an ongoing wide-angle survey for optically bright ($B \leq 17.5$) QSOs in the southern hemisphere, based on digitized objective prism plates taken with the ESO Schmidt telescope (Wisotzki et al. 1996). QSO candidates are selected with a wide range of criteria and followed up spectroscopically with ESO telescopes. The object HE 1127−1304 was first observed as a regular QSO candidate on 1996 March 20, and identified as a QSO with emission redshift $z = 0.63$. The coordinates are R.A. $11^{\rm h}30^{\rm m}19^{\rm s}.9$, Dec. $-13^{o}20'51''$ (J2000). The blue magnitude is $B_J = 16.35$ as measured in the calibrated photographic data.

⋆E-mail: sanjay@ncra.tifr.res.in(SB); krishna@ncra.tifr.res.in(G-K); st2b307@hs.uni-hamburg.de(LW)

2 OBSERVATIONS

2.1 Radio observations

The radio imaging was carried out at 4.9 GHz using the Very Large Array (VLA) in the B/C hybrid configuration, using a bandwidth of 50 MHz. A 10-min snapshot was taken and phase calibrated using the source 1130–148. The flux scale was set using 3C48 and 3C286 on the flux density scale defined by Baars et al. (Baars et al. 1977). The CLEANed map, self-calibrated for phase, and restored with a beamwidth of 7×1.8 arcsec^2 is shown in Fig. 1. It reveals a three-component structure, the parameters of which are summarized in Table 1. The integrated flux density of the source in this 4.9-GHz map is 290 ± 19 mJy which is comparable within errors to the value 270 mJy at 5 GHz given in the Parkes catalogue. The unresolved central peak coincides to within 1 arcsec with the optical position of the QSO with $z = 0.6337$ (Section 2.2). Earlier, based on a less precise radio position, Bolton, Shimmins & Wall (1975) had identified this source with an 18.5-mag galaxy.

The separation between the outermost radio peaks is 296.8 arcsec, which translates to 2.37 Mpc, taking $H_0 = 50$ km s^{-1} Mpc^{-1} and $q_0 = 0.5$. The excellent alignment of the two outer components with the unresolved central component virtually guarantees their physical association. This is further supported by (i) the lengthy jet-like feature extending from the western hotspot towards the central component, and (ii) the presence of diffuse inward

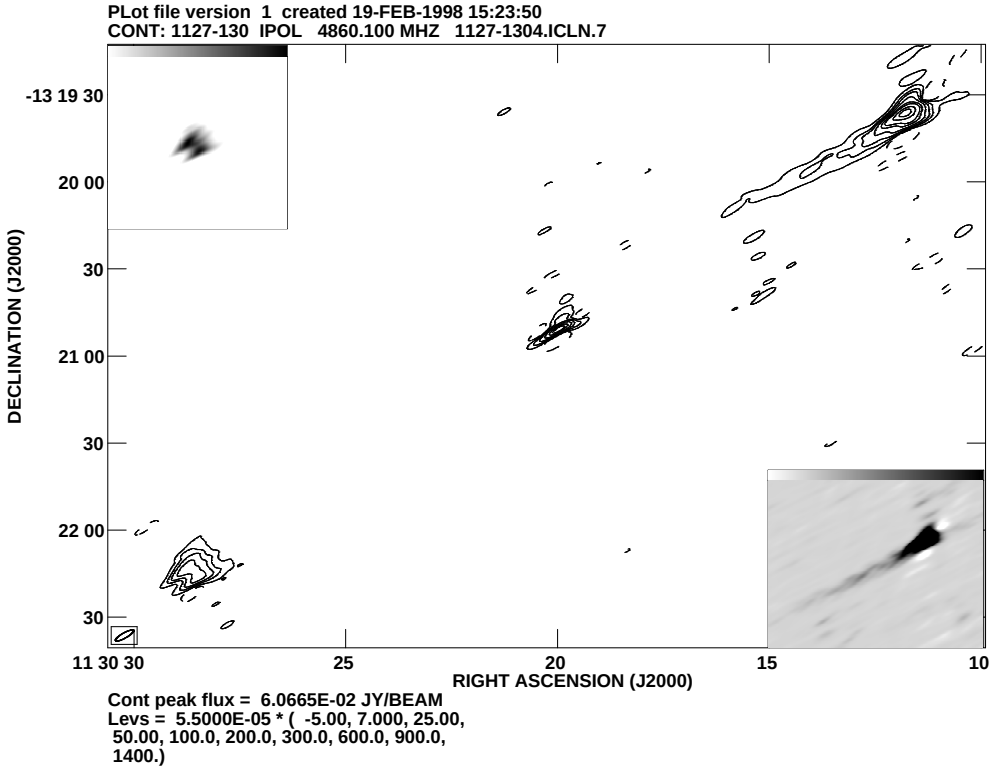

Figure 1. Total intensity VLA map with a beam of 7×1.8 arcsec^2 ($-60°$) at 4.9 GHz. RMS noise is 60 μJy beam^{-1}. The insets in the top left and bottom right corners show the grey-scale images of the south-eastern and north-western lobes, respectively.

extensions in each lobe, seen on the 1.4-GHz VLA map extracted from the NRAO–VLA Sky Survey data base (Condon et al. 1998; Fig. 2). Note that this map, with a modest resolution of 45 arcsec, has an integrated source flux density of 1142 mJy at 1.4 GHz. The source is also listed in the Molonglo catalogue (Large et al. 1981), with a flux density of 2.53 ± 0.13 Jy, which is likely to be a substantial underestimate in view of the source size being comparable to the 3-arcmin beam of the Molonglo map. These integrated flux densities imply a spectral index of about -0.87 for this quasar ($S_\nu \propto \nu^\alpha$). The spectral indices of the individual components, based on the 4.9-GHz VLA and the 1.4-GHz NVSS maps (Figs 1 and 2) are given in Table 1. Note that owing to the large beamwidth of the NVSS map at 1.4 GHz, the peak flux density measured at the position of the compact central component is likely to have some contribution from any adjacent diffuse features. Consequently, the spectum of the central component is probably even flatter than implied by $\alpha = -0.28$ given in Table 1.

2.2 Optical imaging and spectroscopy

New *R*-band CCD image of the field centred at the quasar was obtained on 1998 February 26, using the ESO 3.6-m telescope equipped with EFOSC2 (Fig. 3). Exposure time was 2 min, at a seeing of 1.4 arcsec and a pixel size of 0.32 arcsec. The image was debiased and flat-fielded in the standard way. Aperture photometry gives a magnitude of $R = 15.98$ for the quasar, based on an observation of the standard star GD 108 directly before.

Improved low- and medium-resolution spectra were also taken

Table 1. The parameters of HE 1127–1304.

	Integrated	Comp A (Eastern)	Central Comp	Comp B (Western)
α_{2000}	–	11 30 28.59	11 30 19.98	11 30 11.79
δ_{2000}	–	−13 22 12.9	−13 20 51.0	−13 19 36.2
$S_{4.9}$ (mJy)	290	48.9	25.6	213.1
$S_{1.4}$ (mJy)	1142	251	18.2	865
$\alpha_{1.4}^{4.9}$		−1.31	−0.28	−1.13
LAS($''$)	296.8	–		–
m_R	–	–	15.98	–
m_B	–	–	16.35	–
M_B	–		−25.88	–
z	–	–	0.6337	–
Size (Mpc)	2.37	–	–	–

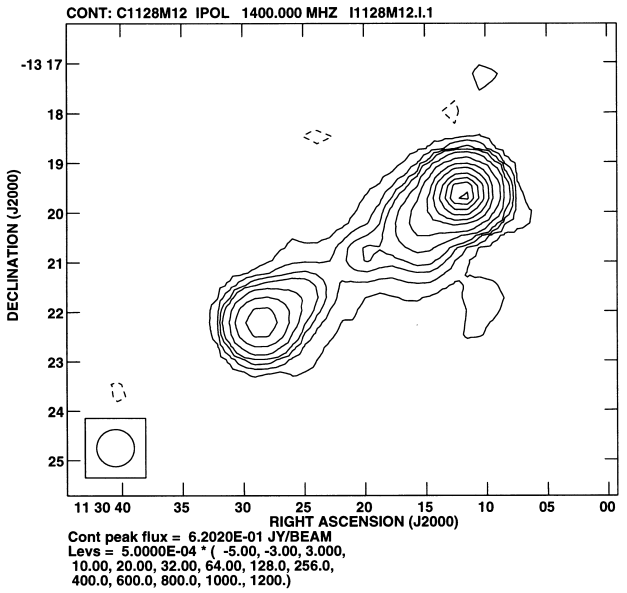

Figure 2. Total intensity NVSS map with a beam of 45×45 arcsec^2 at 1.4 GHz. RMS noise is 0.6 mJy beam^{-1}.

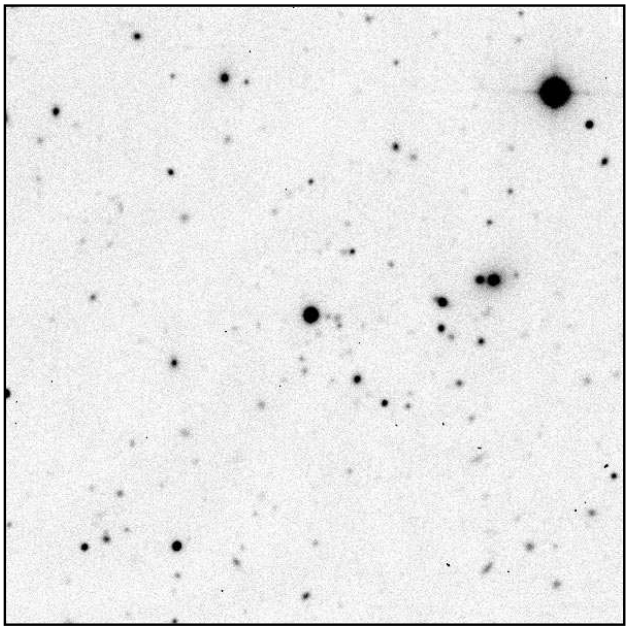

Figure 3. The *R*-band optical image of the field around the QSO taken on 1998 February 26, using the ESO 3.6-m telescope equipped with EFOSC2. The image is 3×3 arcmin^2 centred on the quasar.

on 1998 February 26, using EFOSC2 at the 3.6-m telescope (Fig. 4). The B300b grism with a 1 arcsec slit gave a spectral resolution of ~8 Å (FWHM), while the B150 grism permitted 3.6-Å resolution. The spectra were reduced as usual, including wavelength calibration from a helium–argon lamp and relative flux calibration using wide-slit measurements of the Hubble Space Telescope standard star GD 108. Because of the narrow slit and the conditions which were not strictly photometric, no absolute flux calibration was attempted.

The discovery spectrum (not shown here) displays also Hβ and [O III] $\lambda\lambda$5007, 4959 doublet, yielding an emission redshift of $z_{em} = 0.6337 \pm 0.0002$, which should represent the systemic redshift quite accurately.

3 DISCUSSION

A vast majority of the giant radio sources reported so far are identified with galaxies (see Saripalli et al. 1986; Subrahmanyan et al. 1996; Cotter et al. 1996 and references therein). The two giant quasars reported in the literature are: 4C34.47 ($z = 0.2055$: Jägers et al. 1982, Barthel 1987) and 4C74.26 ($z = 0.104$: Riley et al. 1988, Riley & Warner 1990). Their radio extents are 1.8 and 1.5 Mpc, respectively. Two other giant radio sources, namely 0309+411 (de Bruyn 1989) and 1626+515 (Röttgering et al. 1996), albeit reported as galaxies, show evidence for a broad component of $H\alpha$ emission line, based on the spectra presented in the discovery papers. Therefore, they could well be classified as quasars. Their radio sizes are 1.8 and 1.6 Mpc, respectively. Thus, with a size of 2.4 Mpc, the quasar HE 1127–1304, reported here, is the largest known radio source associated with a quasar, and the only quasar known to have a projected size exceeding 2 Mpc. It is also the most distant giant radio quasar known; all the five giant radio sources found at still larger distances are galaxies (see Cotter et al. 1996; Lacy et al. 1993).

The high-resolution VLA maps of all the five giant quasars mentioned above exhibit a clear asymmetry in the brightness of their lobe extremities (i.e. hotspots). In each case, the brighter hotspot is seen to be on the side of the jet. A similar trend has been noticed earlier for normal size quasars, with a high degree of statistical significance (Laing 1989; Bridle et al. 1994). The frequent appearance of a more prominent hotspot on the jetted side is commonly attributed to the same Doppler favouritism which is invoked to explain the asymmetry of the jet (Laing 1989). The conformity of all the GRQs to this pattern shows that even out to almost a megaparsec from the nucleus, jets are able to sustain relativistic bulk motion, resulting in a relativistic post-shock outflow of the synchrotron plasma within the hotspots. Note that this signature for relativistic jet flow in the *giant* quasars is even more remarkable, given that any orientation-dependent effects are expected to be weaker in view of the adopted selection criterion of a very large projected size. In our VLA map of HE 1127–1304, the fainter hotspot which is associated with the eastern radio lobe located on the counter-jet side is resolved into two peaks of comparable brightness (Fig. 1). Double hotspots are not uncommon for radio lobes and, conceivably, these could be a result of non-axisymmetric shocks in the jets, leading to their deflection after the first shock (e.g. Laing 1989). A map of the eastern lobe of HE 1127–1304, with better resolution and dynamic range, is needed to clarify the nature of its brightness peak. This is also of interest in the context of an alternative scenario, in which a pair of warm spots straddling a narrow region of depressed emission can be the result of Doppler dimming of the putative hotspot of a receding lobe, while the two sides of the same hotspot appear as warm spots produced by the Doppler-beamed, backward-flowing synchrtron plasma (see Tribble 1992).

The optical spectrum of the quasar clearly shows a broad emission line of Mg II λ2798 (rest frame FWHM 16 700 km s^{-1}; Fig. 4). Note that the broad Mg II emission line is blueshifted by 2400 km s^{-1} with respect to the systemic velocity reference (i.e. Hβ and [O III] lines; Section 2.2).

An even more striking spectral feature is the deep absorption seen superimposed on the broad Mg emission line. In the 3.6-Å

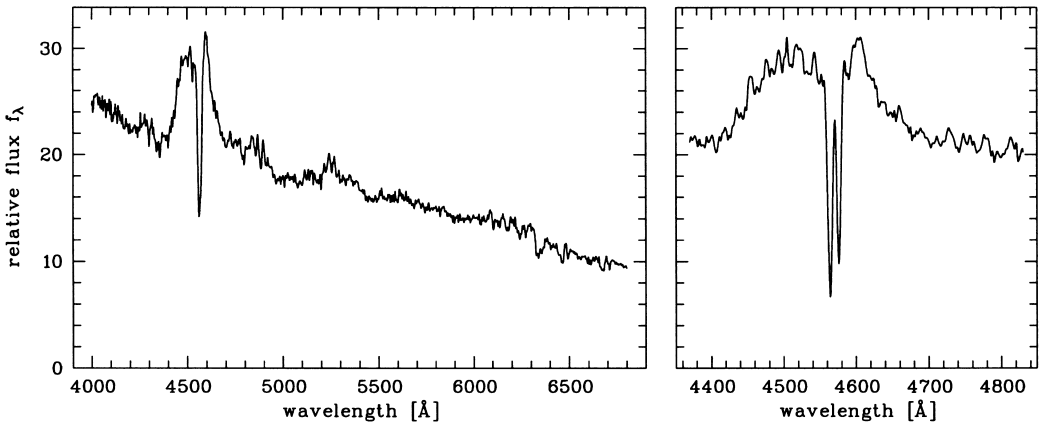

Figure 4. Medium (∼8 Å) and high (3.6 Å) resolution spectra clearly showing the deep Mg II λ2798 absorption feature(s) superposed on the broad Mg II emission line (see Section 2.2).

resolution spectrum, the absorption feature is resolved into the two components of the Mg II λλ2796, 2803 doublet, although the individual absorption lines are unresolved (Fig. 4). There is some indication of an additional absorption component at slightly shorter wavelengths, but the spectral resolution is insufficient to allow us to obtain the details. The absorption redshift $z_{abs} = 0.6337 \pm 0.0001$ is blueshifted by ∼300 km s^{-1} relative to the adopted reference. The rest frame equivalent width of the Mg II absorption feature is ∼10 Å – a more accurate value cannot be determined at the given spectral resolution, as the intrinsic profile of the broad emission line is unknown. We have assumed a flat-topped emission profile, so our estimate of the equivalent width is rather a lower limit. Yet, this is clearly an extreme value, even considering the reported tendency for associated Mg absorption to be stronger in steep-spectrum quasars (Aldcroft, Bechtold & Elvis 1994).

4 CONCLUSIONS

During an ongoing radio follow-up of the Hamburg–ESO optical survey for quasars, we have discovered a 2.4-Mpc long triple radio source associated with a quasar at $z = 0.6337$. This is the largest and the most distant among the giant radio quasars reported so far. Its radio lobe morphology is consistent with bulk motion of the jet persisting to megaparsec scale. The optical spectrum of this quasar is marked by two exceptionally deep absorption features of the Mg II λλ2796, 2803 doublet.

5 ACKNOWLEDGMENTS

The VLA is operatred by the National Radio Astronomy Observatory (NRAO) for Associated Universities Inc. under a licence from the National Science Foundation of the USA. It is a pleasure to thank Professor V. K. Kulkarni and Dr Jayaram N. Chengalur for the helpful discussions. We also thank Dr A. Schoenmaker and Dr G. Cotter for informative communications.

REFERENCES

Aldcroft T. L, Bechtold J., Elvis M., 1994, ApJS, 93, 1
Baars J. W. M., Genzel R., Pauliny-Toth I. I. K., Witzel A., 1977, A&A, 61, 99
Barthel P. D., 1987, in Zensus J. A., Perason T. J., eds, Superluminal Radio Sources. Cambridge Univ. Press, Cambridge, p. 148
Barthel P. D., 1989, ApJ, 336, 606
Bolton J. G., Shimmins A. J., Wall J. V., 1975, Austral. J. Phys., Ap.Suppl., 34, 1
Bridle A. H., Hough D. H., Lonsdale C. J., Burns J. O., Laing R. A., 1994, AJ, 108, 766
Condon J. J., Cotton W. D., Greisen E. W., Yin Q. F., Perley R. A., Taylor B., Broderick J. J., 1998, AJ, 115, 1693
Cotter G., Rawlings S., Saunders R., 1996, MNRAS, 281, 1081
de Bruyn A. G., 1989, A&A, 226, L13
Gopal-Krishna, Witta P. J., Saripalli L., 1989, MNRAS, 239, 173
Jägers W. J., van Breugel J. M., Miley G. K., Schilizzi R.T., Conway R. G., 1982, A&A, 105, 278
Lacy M., Rawlings S., Saunders R., Warner P.J., 1993, MNRAS, 264, 721
Laing R. A., 1989, in Meisenheimer K., Röser H. -J., eds, Hot Spots in Extragalactic Radio Sources. Springer, Berlin, p. 27
Large M. I., Mills B. Y., Little A. G., Crowford D. F., Sutton J. M., 1981, MNRAS, 194, 693
Riley J. M., Warner P. J., 1990, MNRAS, 246, 1P
Riley J. M., Warner P. J., Rawlings S., Saunders R., Pooley G. G., Eales S. A., 1988, MNRAS, 236, 13P
Röttgering H. J. A., Tang Y., Bremer M. A. R., de Bruyn A. G., Miley G. K., Rengelink R. B., Bremer M. N., 1996, MNRAS, 282, 1033
Saripalli L., Gopal-Krishna, Reich W., Kühr H., 1986, A&A, 170, 20
Saunders R., 1982, PhD thesis, Univ. Cambridge
Subrahmanyan R., Saripalli L., 1993, MNRAS, 260, 908
Subrahmanyan R., Saripalli L., Hunstead R. W., 1996, MNRAS, 279, 257
Tribble P., 1992, MNRAS, 256, 281
Willis A. G., Strom R. G., Wilson A.S., 1974, Nat, 250, 625
Wisotzki L., Köhler T., Groote D., Reimers D., 1996, A&AS, 115, 227

This paper has been typeset from a TEX/LATEX file prepared by the author.